JACS
JOURNAL OF THE AMERICAN CHEMICAL SOCIETY
Communication
pubs.acs.org/JACS

Mechanisms of Stereomutation and Thermolysis of Spiro-1,2-oxaphosphetanes: New Insights into the Second Step of the Wittig Reaction

Jesús García López,[†] Antonio Morán Ramallal,[‡] Javier González,*[,‡] Laura Roces,[§] Santiago García-Granda,[§] María José Iglesias,[†] Pascual Oña-Burgos,[†] and Fernando López Ortiz*[,†]

[†]Área de Química Orgánica, Universidad de Almería, 04120 Almería, Spain
[‡]Departamento de Química Orgánica e Inorgánica, Universidad de Oviedo, C/Julián Clavería 8, 33006 Oviedo, Spain
[§]Departamento de Química Física y Analítica, Universidad de Oviedo-CINN, C/Julián Clavería 8, 33006 Oviedo, Spain

Supporting Information

ABSTRACT: The experimentally observed stereomutation of spiro-1,2-oxaphosphetanes is shown by DFT calculations to proceed through successive M_{B2} or M_{B4} and M_{B3} mechanisms involving two, four, and three Berry pseudorotations at phosphorus, respectively. Oxaphosphetane decomposition takes place in a single step via a polar transition state. The calculated activation parameters for this reaction are in good agreement with those determined experimentally.

The Wittig reaction is the most popular method for introducing double bonds at specific positions of organic molecules.[1a,c] The generally accepted mechanism involves three stages:[1b] asynchronous [2 + 2] cycloaddition to give an oxaphosphetane (OPA, **I**), pseudorotation at phosphorus to form an anti-apicophilic P−O_{eq} isomer (**III**),[2] and asynchronous [2 + 2] cycloreversion to yield the olefin and phosphine oxide (Scheme 1). Although some anti-apicophilic OPAs have been isolated,[3] they convert into the P−O_{ap} isomer during decomposition.[3b] Recent ab initio calculations on realistic Wittig reactions suggested that **III** is not an intermediate in the reaction pathway.[4] Isomerization of P−O_{ap} OPAs (**I** ⇄ **II**) is also known. In typical OPAs, this stereomutation is much faster than fragmentation.[5] The activation free energy ($\Delta G^{\ddagger}$) for OPA interconversion in spirodibenzophosphole (spiro-DBP) derivatives (13.1−14.6 kcal mol^{-1}) is ca. 10 kcal mol^{-1} lower than the $\Delta G^{\ddagger}$ for decomposition.[5a,b] In special cases, OPA decomposition may be faster than stereomutation.[6]

Scheme 1. Possible Stereomutation Mechanisms in the Wittig Reaction

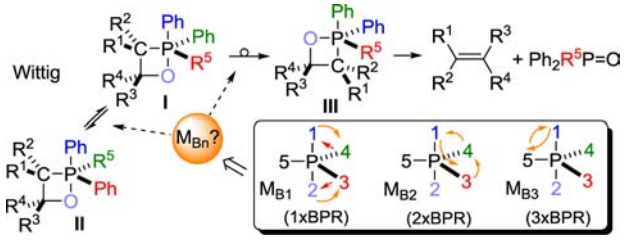

The positional interchange of apical (ap) and equatorial (eq) ligands in the trigonal bipyramid (TBP) geometry of OPAs has been described as a Berry pseudorotation[7] (BPR) or turnstile rotation[8] (TR).[1,9] Very recently,[10] it has been shown that isomerization of TBPs may occur in three ways: BPR, threefold cyclic permutation, and half-twist ap−eq interchange (M_{B1}, M_{B2}, and M_{B3}, respectively). These are one-step processes, and the subscript indicates the number of BPRs involved (Scheme 1).[11] TR has been proved to be equivalent to BPR. The comments above indicate that the role and mechanism of stereomutation in the Wittig reaction remain unclear. Addressing this issue is hampered by the instability of the substrates. The rate of ap−eq exchange can be decreased using bidentate ligands.[5b,c,9,12] Herein we describe a study of the isomerization and thermal decomposition of isolable spiro-1,2-oxaphosphetanes. Key features of this study are (1) the synthesis of enantiopure derivatives, (2) the identification of three mechanisms of OPA stereomutation (M_{B2}, M_{B3}, and a new one labeled as M_{B4}), and (3) the description of olefination as a single-step reaction.

Spiro-oxaphosphetanes **2**−**6**, which are stabilized by the presence of the *o*-benzamide (*o*BA) moiety, were synthesized using previously reported procedures (Table 1).[13] The reactions with the hindered ketone L-(−)-camphor (technical grade, ca. ∼70% ee) gave products **5** and **6** (90% conversion, 45:55 ratio; entries 4 and 5) arising from endo attack at the CO group of L-camphor. They were separated through semi-preparative HPLC. Recrystallization of **6** (72% ee) from toluene furnished crystals of (±)-**6** suitable for X-ray diffraction (XRD) [Figure S27 in the Supporting Information (SI)] and (+)-**6** (>97% ee). The corresponding reactions with D-(+)-camphor (>97% ee) gave rise to enantiopure *ent*-**5** and *ent*-**6** (Figures S7 and S8).

Thermal decomposition of OPAs **2**−**6** afforded alkenes **7**−**11** and heterocycle **12** quantitatively (Table 1). In the thermolysis of **3**−**6**, partial isomerization to **3′**−**6′** having the configuration of the P atom inverted was observed (Table 1, Tables S4 and S5 in the SI, and Figure S14). The new products were characterized in situ by NMR spectroscopy (Figure S14).

Received: July 26, 2012
Published: November 20, 2012

   dx.doi.org/10.1021/ja307330c | J. Am. Chem. Soc. 2012, 134, 19504−19507

Table 1. OPAs 2−6, Decomposition Products 7−11, and P═O Byproduct 12

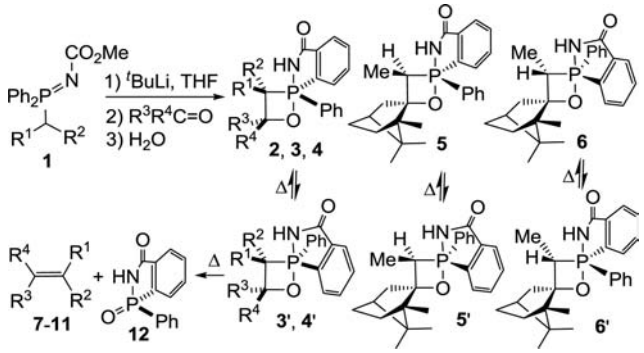

entry	comp.	R^1	R^2	R^3	R^4	yield (%)
1	**2**	Me	Me	Ph	Ph	85
2	**3** (**3'**)	Me	H	$(CH_2)_5$		82 (2.6)[a]
3	**4** (**4'**)[b]	Me	Me	Me	Ph	89 (32.7)[a]
4	**5**[c] (**5'**)	Me	H			44 (2.0)[a]
5	**6**[c] (**6'**)	H	Me			22 (7.3)[a]
6	**7**	Me	Me	Ph	Ph	100
7	**8**	Me	H	$(CH_2)_5$		100
8	**9**	Me	Me	Me	Ph	100
9	**10**[c]	Me	H			100
10	**11**[c]	H	Me			100

[a]Conversion of permutational isomers **3'**−**6'** was observed by ^{31}P NMR spectroscopy. [b]Characterized in ref 13. [c]*ent*-**5**/**6** and *ent*-**10**/**11** were prepared from D-(+)-camphor (>97% ee).

In the decomposition of enantiopure **6** (THF, 7 days!), this stereomutation led to partially racemized **12** (80% ee; Scheme 2).[14] The collapse of **5** (84% ee)/*ent*-**5** (>97% ee) to the final products was achieved in only 15 h. Recrystallization of the P═O byproduct from toluene furnished optically pure (S_P)-**12**. The configuration was assigned by XRD analysis (Figure S28). The stereospecific formation of alkenes **10** and **11** ruled out the existence of stereochemical drift (reversible OPA opening/recombination). As far as we know, this is the first time that the stereochemical course of the P stereocenter has been ascertained in the decomposition of an enantiopure OPA. McEwen et al.[6a] reported that the Wittig reaction of (+)-EtMePhP═CHPh with benzaldehyde proceeds stereospecifically with retention of configuration of the P atom (i.e., decomposition is faster than stereomutation). The results were explained in terms of the participation of three possible OPAs of TBP and square pyramid (SP) geometry.

Scheme 2. Decomposition of Spiro-OPAs 5 and 6

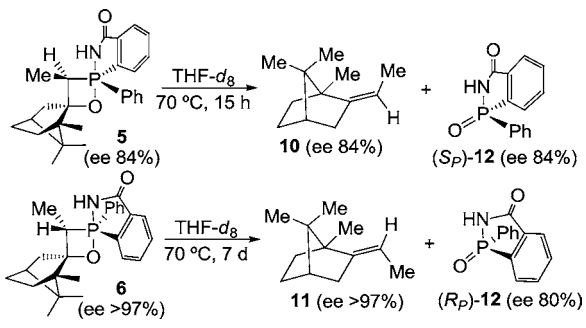

Since decomposition and stereomutation are concurrent processes, we determined the activation parameters for the thermolysis of **2**, where only the latter is observed. The kinetics of olefin formation in toluene was investigated by ^{31}P NMR spectroscopy. The reaction was first order in the oxaphosphetane. The temperature dependence of k led to an estimation of the activation parameters as $\Delta H^{‡} = 30.4 \pm 0.6$ kcal mol^{-1} and $\Delta S^{‡} = -1.3 \pm 1.4$ cal mol^{-1} K^{-1} (see the SI), which gave $\Delta G^{‡} = 30.9 \pm 1.1$ kcal mol^{-1} at $T = 403.15$ K. This activation barrier is >10 kcal mol^{-1} higher than those for typical OPAs[1,5,9] and slightly lower than those for disubstituted spiro-oxaphosphetanes stabilized by the Martin ligand.[15]

The mechanism of olefination of oxaphosphetanes **2**, **5**, and **6** was studied using density functional theory at the B3LYP/6-31G* level. The validation of the method is described in the SI. The potential energy surface (PES) of **2** consists of seven stationary points: energy minima for OPAs **2** and **2″**, alkene **7**, and benzoazaphosphol **12** and the respective transition states (TSs) for fragmentation ([**2**·**A**]‡ and [**2″**·**A**]‡) and stereomutation ([**2**·**B**]‡) (Figure 1 and Table S6). **2** and **2″** are permutational isomers showing distorted TBP geometries. **2** is 6 kcal mol^{-1} more stable than **2″**, which supports the exclusive detection of **2** in solution. Isomerization of **2** into **2″** proceeds through [**2**·**B**]‡ (barrier of 24.4 kcal mol^{-1}), which has a TBP-like geometry with the O1, N, and C8 atoms in the equatorial plane and C3 and C13 in apical positions (Figure S17). The negative $\Delta S^{‡}$ of −6.9 cal mol^{-1} K^{-1} is assigned to steric strain induced by ligand interchange.[5c] The calculated $\Delta G^{‡}$ of stereomutation is ca. 10 kcal mol^{-1} higher than that experimentally obtained for DBP-stabilized spiro-OPAs.[5a,b]

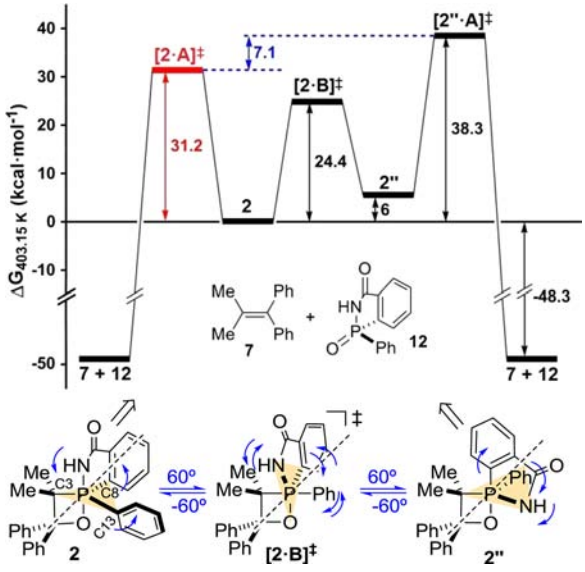

Figure 1. Energy profile of the decomposition of **2** and stereomutation via the M_{B2} mechanism.

dx.doi.org/10.1021/ja307330c | J. Am. Chem. Soc. 2012, 134, 19504−19507

This difference in $\Delta G^{\ddagger}$ can be assigned to the larger stabilization provided by the *o*BA ligand compared with the DBP moiety. The process **2** ⇄ **2″** can be described as a 120° cyclic rotation of one apical and two equatorial ligands (i.e., an M_{B2} mechanism; Figure 1).[10,11] The imaginary vibrational mode of [**2·B**]‡ supports this conclusion. To the best of our knowledge, this is the first report of the interconversion of OPAs by the M_{B2} mechanism.

The decomposition of **2** is a single-step, highly exothermic, irreversible reaction (Figure 2) with a barrier of 31.2 kcal mol^{-1}

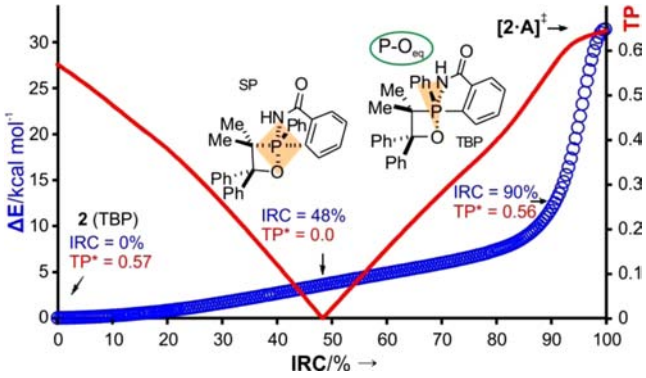

Figure 2. Graph of relative energy ΔE (blue ○) and TP (red line) along the IRC for the decomposition of **2**.

and a small negative entropy of −2.7 cal mol^{-1} K^{-1} (Table S6), in excellent agreement with the activation parameters obtained in toluene. **2** decomposes in an asynchronous concerted process via [**2·A**]‡. The normal mode of the imaginary frequency of this TS corresponds to dissociation of the P−C3 and C4−O1 bonds (with the former being more advanced than the latter) and formation of the C3−C4 and P−O1 double bonds. [**2·A**]‡ shows a TBP geometry with C3 and C8 in apical positions, indicating that ring opening involves P pseudorotation (the O1−P−N angle decreases from 170.7 to 129° and the C3−P−C8 angle increases from 124.8 to 167.7°).

In contrast to the generally accepted mechanism of the second step of the Wittig reaction,[1b,c,2] at the level of computation used, positional exchange of the ligands is predicted to take place along the reaction coordinate leading to [**2·A**]‡ without the participation of an anti-apicophilic P−O_{eq} intermediate. This finding is supported by recent ab initio calculations.[4] A TBP structure containing a P−O_{eq} bond was found at an internal reaction coordinate (IRC) of 90% in the cycloreversion reaction (Figure 2). The V-shaped pattern of the topology parameter (TP)[16] connecting this point with **2** is characteristic of a Berry stereomutation. Analogously, the decomposition of **2″** proceeds through [**2″·A**]‡ to give **7** and **12** and is disfavored by 7.1 kcal mol^{-1} relative to that of **2**.

The computational study was extended to **5** and **6** to explain why **6**, with the *R* configuration at the P atom, decomposes with partial racemization of **12** at a rate that is ca. 20 times lower than for **5**. The PES for the decomposition of **6** includes OPAs **6**, **6′**, and **6″** and products **11** and **12** (Table S9). Solvent effects were estimated by using the polarized continuum model (PCM). The geometrical parameters calculated for **6** are in excellent agreement with those experimentally determined for (±)-**6** [e.g., the bond distances in the OPA ring for the isolated/calculated structures are P−O1 1.724(3)/1.773, P−C3 1.821(4)/1.870, C3−C4 1.535(5)/1.555, and C4−O1 1.453(5)/1.446 Å, and the N−P−O1 bond angles are 166.63(15)°/165.4°]. The motion of the P substituents of **6** may follow two courses. Two consecutive 60° clockwise rotations of the N, C8, and C13 ligands (M_{B2} mechanism) convert **6** into **6″** via TS [**6·B**]‡ having a TBP geometry (barrier of 24.2 kcal mol^{-1}; Figure 3 and Figures S21−S23).

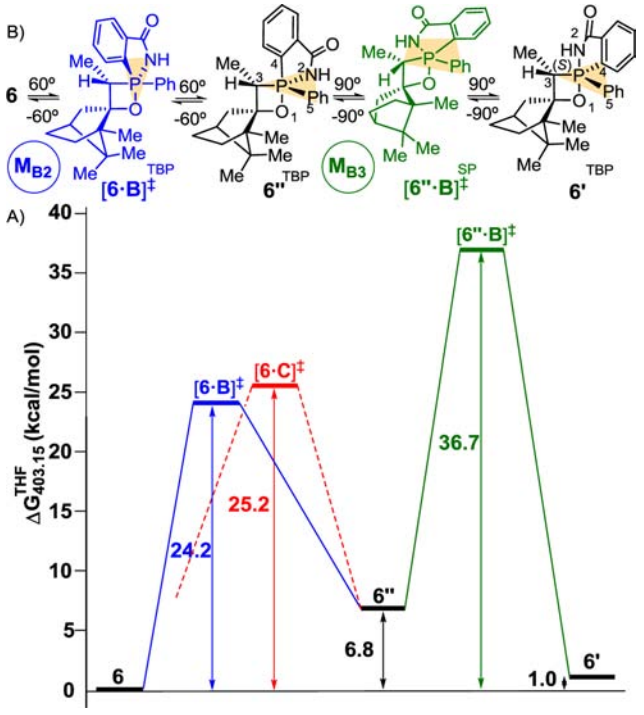

Figure 3. (A) Energy profile for the **6** ⇄ **6″** ⇄ **6′** interconversion. (B) Minimum-energy pathway involving the M_{B2} and M_{B3} mechanisms.

Most importantly, two successive 120° anticlockwise rotations produce the same isomerization through the new TS [**6·C**]‡ having a TBP configuration with O1 and C13 in apical positions. This process involves four BPRs and represents a new mechanism of stereomutation identified as M_{B4}. The barrier is only 1 kcal mol^{-1} higher than that of the M_{B2} mechanism, which makes M_{B4} a reasonable alternative for the **6** ⇄ **6″** interconversion.

The validity of the MB4 mechanism is supported by the analysis of the TP for this stereomutation.[10] A plot of the TP along the IRC shows the expected quadruple-V-shaped pattern (Figure 4). The discontinuity observed is due to differences between bond angles arising from the lack of symmetry of the system. The four local vertexes correspond to structures having SP geometry (TP = 0.0) and the three local cusps are TBP structures characterized by TP values in the range 0.45−0.75 (Figure S25). This analysis shows that the new M_{B4} mechanism complements the description of stereomutation in TBP structures proposed by Lammertsma and co-workers[10] as single-step processes involving a number of BPRs.

Interchange of the C8 and N ligands in **6″** through a 180° rotation leads to **6′**, the isomer of **6** experimentally observed via P stereomutation. The TSs for this process, [**6″·B**]‡ and [**6″·C**]‡, arise from clockwise and anticlockwise rotations, respectively (Figure S24). Both TSs have SP geometry and are located halfway through three consecutive Berry pseudorotations, as expected for an M_{B3} mechanism.[10] Stereomutation through [**6″·B**]‡ is highly favored because its barrier (30 kcal mol^{-1})[17] is 7.1 kcal mol^{-1} lower than that of [**6″·C**]‡. A Levi−

dx.doi.org/10.1021/ja307330c | J. Am. Chem. Soc. 2012, 134, 19504−19507

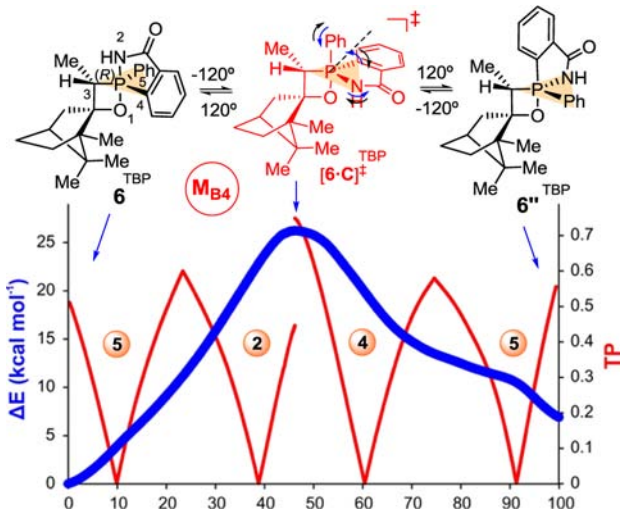

Figure 4. Graph of relative energy Δ*E* (blue) and TP (red) along the IRC for the **6** ⇄ **6″** stereomutation via the MB4 mechanism. Pivot atom assignments are shown.

Desargues[18] graphical representation of the **6** ⇄ **6″** ⇄ **6′** isomerization is shown in Figure S26.

The barrier for olefination of **6** (29.9 kcal mol^{-1}) is 0.5 and 6.8 kcal mol^{-1} lower than those for decomposition of **6′** and the **6** ⇄ **6′** interconversion, respectively. The unfavorable formation of **6′** may be accelerated by the presence of acidic species in the reaction medium (e.g., **12**).[3b,19] The detection of **6′** only after 57.5 h of heating supports this assumption. Importantly, **5** is destabilized by 5.1 kcal mol^{-1} with respect to **6**, and the barrier for cycloreversion (27.3 kcal mol^{-1}) is 1.7 kcal mol^{-1} lower than for **6**. The destabilization of **5** arises from the interaction of the C3-Me protons with the camphor moiety (Figure S15).

In summary, this study of the decomposition of isolable spiro-1,2-oxaphosphetane intermediates in a Wittig-type reaction allowed us to determine the activation parameters for the process; to characterize the cycloreversion as a single-step concerted asynchronous reaction that irreversibly affords the corresponding alkene and P byproduct via a polar TS; and to describe for the first time the stereomutation through three possible mechanisms MB2, MB3, and MB4 involving two, three, and four Berry pseudorotations, respectively. The MB4 mechanism is unprecedented and contributes to completing the description of the motion of substituents in the interconversion of pentacoordinated species having TBP geometry.[10,11]

■ ASSOCIATED CONTENT

Supporting Information

Experimental and computational details, characterization data, rate constants measured, Cartesian coordinates and energies of the stationary points located, and crystallographic data for (±)-**6** and (*S*$_P$)-**12** (CIF). This material is available free of charge via the Internet at http://pubs.acs.org.

■ AUTHOR INFORMATION

Corresponding Author

flortiz@ual.es; fjgf@uniovi.es

Notes

The authors declare no competing financial interest.

■ ACKNOWLEDGMENTS

Dedicated to Prof. F. J. Palacios on the occasion of his 60th birthday. This work was supported by the Ministerio de Ciencia e Innovación and the FEDER Program (Projects CTQ2008-117BQU, CTQ2011-27705, MAT2010-15094, PTA-2009-2346-I, and CSD2006-015, Consolider Ingenio 2010, "Factoría de Crystalización").

■ REFERENCES

(1) For a review, see: (a) Vedejs, E.; Peterson, M. J. *Adv. Carbanion Chem.* **1996**, *2*, 1. Recent references: (b) Robiette, R.; Richardson, J.; Aggarwal, V. K.; Harvey, J. N. *J. Am. Chem. Soc.* **2006**, *128*, 2394. (c) Byrne, P. A.; Gilheany, D. G. *J. Am. Chem. Soc.* **2012**, *134*, 9225.

(2) (a) Höller, R.; Lischka, H. *J. Am. Chem. Soc.* **1980**, *102*, 4632. (b) Bestmann, H. J.; Chandrasekhar, J.; Downey, W. G.; Schleyer, P. v. R. *J. Chem. Soc., Chem. Commun.* **1980**, 978.

(3) (a) Vollbrecht, S.; Vollbrecht, A.; Jeske, J.; Jones, P. G.; Schmutzler, R.; du Mont, W.-W. *Chem. Ber.* **1997**, *130*, 819. (b) Kojima, S.; Sugino, M.; Matsukawa, S.; Nakamoto, M.; Akiba, K.-y. *J. Am. Chem. Soc.* **2002**, *124*, 7674. (c) Kobayashi, J.; Kawashima, T. *C. R. Chim.* **2010**, *13*, 1249.

(4) (a) Lu, W. C.; Wong, N. B.; Zhang, R. Q. *Theor. Chem. Acc.* **2002**, *107*, 206. (b) Seth, M.; Senn, H. M.; Ziegler, T. *J. Phys. Chem. A* **2005**, *109*, 5136. (c) Alagona, G.; Ghio, C. *Theor. Chem. Acc.* **2009**, *123*, 337. (d) Alagona, G.; Ghio, C. *Int. J. Quantum Chem.* **2010**, *110*, 765.

(5) (a) Vedejs, E.; Marth, C. F. *J. Am. Chem. Soc.* **1989**, *111*, 1519. (b) Vedejs, E.; Marth, C. F. *J. Am. Chem. Soc.* **1990**, *112*, 3905. (c) Bangerter, F.; Karpf, M.; Meier, L. A.; Rys, P.; Skrabal, P. *J. Am. Chem. Soc.* **1998**, *120*, 10653.

(6) (a) McEwen, W. E.; Kumli, K. F.; Blade-Font, A.; Zanger, M.; VanderWerf, C. A. *J. Am. Chem. Soc.* **1964**, *86*, 2378. (b) Vedejs, E.; Fleck, T. J. *J. Am. Chem. Soc.* **1989**, *111*, 5861.

(7) Berry, R. S. *J. Chem. Phys.* **1960**, *32*, 933.

(8) (a) Ugi, I.; Ramirez, F.; Marquarding, D.; Klusacek, H.; Gokel, G.; Gillespie, P. *Angew. Chem., Int. Ed. Engl.* **1970**, *9*, 725. (b) Ugi, I.; Marquarding, D.; Klusacek, H.; Gillespie, P. *Acc. Chem. Res.* **1971**, *4*, 288.

(9) Vedejs, E.; Marth, C. F. In *Phosphorus-31 NMR Spectral Properties in Compound Characterization and Structural Analysis*; Quin, L. D., Verkade, J. G., Eds.; VCH: New York, 1994; pp 297−313.

(10) Couzijn, E. P. A.; Slootweg, J. C.; Ehlers, A. W.; Lammertsma, K. *J. Am. Chem. Soc.* **2010**, *132*, 18127.

(11) M_{B1}, M_{B2}, and M_{B3} correspond to the M1, M4, and M2 mechanisms proposed by Muetterties. See: (a) Muetterties, E. L. *J. Am. Chem. Soc.* **1969**, *91*, 1636. (b) Muetterties, E. L. *J. Am. Chem. Soc.* **1969**, *91*, 4115. We think that the M_{Bi} nomenclature, in which each mechanism is identified by a subscript B*i* indicating the number (*i*) of BPRs involved, allows a given mechanism to be identified more easily.

(12) For 10-P-5 species, see: (a) Kojima, S.; Kajiyama, K.; Nakamoto, M.; Akiba, K.-y. *J. Am. Chem. Soc.* **1996**, *118*, 12866. (b) Kojima, S.; Nakamoto, M.; Akiba, K.-y. *Eur. J. Org. Chem.* **2008**, 1715. (c) Akiba, K.-y. *Organo Main Group Chemistry*; Wiley: New York, 2011.

(13) García-López, J.; Peralta-Pérez, E.; Forcén-Acebal, A.; García-Granda, S.; López-Ortiz, F. *Chem. Commun.* **2003**, 856.

(14) Thermolysis of enantiopure *ent*-**5** and *ent*-**6** furnished (*S*$_P$)-**12** (>97% ee) and (*R*$_P$)-**12** (80% ee), respectively, together with the corresponding enantiopure olefins *ent*-**10** and *ent*-**11** (Figure S13).

(15) (a) Kawashima, T.; Kato, K.; Okazaki, R. *J. Am. Chem. Soc.* **1992**, *114*, 4008. (b) Kawashima, T.; Kato, K.; Okazaki, R. *Angew. Chem., Int. Ed. Engl.* **1993**, *32*, 869.

(16) The TP defined in ref 10 represents the distortion along a Berry process. The limiting values are 0 (ideal SP) and 1 (ideal TBP).

(17) Similar barriers were found in the stereomutation of 10-P-5 spirophosphoranes. See: Jiang, X.-D.; Matsukawa, S.; Yamamich, H.; Kakuda, K.-I.; Kojima, S.; Yamamoto, Y. *Eur. J. Org. Chem.* **2008**, 1392.

(18) Mislow, K. *Acc. Chem. Res.* **1970**, *3*, 321.

(19) Ramirez, F.; Loewengart, G. V.; Tsolis, E. A.; Tasaka, K. *J. Am. Chem. Soc.* **1972**, *94*, 3531.